PREDICTION OF THE ENERGY ABSORPTION BEHAVIOUR OF LARGE COMPOSITE COMPONENTS SUBJECTED TO IMPACT LOADS – ASSESSMENT OF INDIVIDUAL MECHANISMS AT PLY SCALE

Martin Schwab[1], Heinz E. Pettermann[1]

[1]Institute of Lightweight Design and Structural Biomechanics, Vienna University of Technology,
Getreidemarkt 9, A-1060 Vienna, Austria
Email: mschwab@ilsb.tuwien.ac.at, Web Page: http://www.ilsb.tuwien.ac.at

Keywords: Finite element method, Structural component, Impact energy absorption, Continuum damage mechanics, Shell modelling approach

Abstract
An efficient modelling strategy for simulating impact on structural components built from laminated composites is presented. The utilisation of a multiscale embedding approach in combination with shell element based modelling allows to keep the computational effort within reasonable bounds. Thereby, a highly resolved subsection is placed at the region where impact and associated material nonlinearities are expected to occur. Regions remote from the impact zone are modelled by a common laminate approach. The approach is demonstrated by modelling a composite fan containment casing of a jet engine subjected to fan blade out. The simulations are conducted using an explicit Finite Element Method solver. Detailed insight into the components behaviour during the fan blade out event is gained. Eventually, conclusions drawn from such predictions contribute to improvements in the design of impact loaded composite components.

1. Introduction

Impact on structural components built from laminated composites represents a complex dynamic process. Damage and failure mechanisms arise on small length scales at ply and interface level whereas typical component dimensions are several orders of magnitude larger. Hence, numerical predictions of the impact response of large composite components are challenging and often require exceptional computational resources. The present paper applies advanced methods within the framework of the Finite Element Method (FEM), where an efficient modelling strategy in combination with shell element based discretisation allows the computational effort to be kept within reasonable bounds. Thereby, a multiscale embedding approach is utilised where a highly resolved subsection is placed at the region where impact and associated material nonlinearities are expected to occur. Regions remote from the impact zone are modelled by a common laminate approach. The approach is demonstrated by investigating a composite fan containment casing of a jet engine subjected to fan blade out. The simulations are conducted using the explicit FEM solver Abaqus/Explicit v6.14 (Dassault Systemes Simulia Corp., Providence, RI, USA). Detailed insight into the component's behaviour during the fan blade out event is gained. Eventually, conclusions drawn from such predictions contribute to improvements in the design of impact loaded composite components.

Excerpt from ISBN 978-3-00-053387-7

2. Method

2.1. Modelling - laminate level

Within this work, laminated composites consisting of several layers of fabric plies are considered, where a stacked shell approach (SSA) is utilised, cf. [1]. Thereby, the laminate is modelled as a stack of homogeneous orthotropic plies discretised by individual layers of shell elements. The interfaces between individual plies are modelled using cohesive zone elements (CZEs). This arrangement is schematically depicted in Fig. 1.

Individual constitutive laws for plies and interfaces are used to describe the laminate's constitutive behaviour. Mechanisms associated with intra-ply failure (i.e. matrix cracking, fibre rupture, plasticity like effects) are described within the constitutive law of the shell layers whereas inter-ply failure (i.e. delamination) is modelled by a traction-separation based cohesive zone law. The fabric reinforced plies are modelled as homogeneous orthotropic material in combination with an energy based continuum damage mechanics approach to account for tensile and compressive fibre damage. Furthermore, plastic deformation and damage under shear loading are modelled in order to capture the matrix dominated shear response of the ply. This constitutive model is readily available within the FEM package Abaqus/Explicit as a built-in VUMAT user subroutine (ABQ_PLY_FABRIC), cf. [2]. A summary of this material model is also given in Ref. [3]. The interface constitutive response is modelled using the Abaqus built-in traction-separation based constitutive model for CZEs, cf. [4], where damage initiation is predicted according to a quadratic nominal stress criterion and damage evolution is modelled based on the critical energy release rate of the interface in combination with a linear softening relation.

2.2. Modelling - component level

Although the described SSA is proven to be very efficient in terms of computational resources, cf.[1], the application of the SSA to entire components still leads to very demanding FEM models. Considering the case of transverse impact, the domain where material nonlinearities are encountered is limited to the region in the proximity of the impact zone. Within this region, the laminate needs to be modelled sufficiently detailed. Regions remote from the impact zone, which are subject to elastic deformations only, can be modelled less detailed. Within the present work, the SSA is used to model the subsection of the component where impact is expected to occur. This highly resolved subsection is embedded into the surrounding domain, which is represented by a single layer of shell elements and linear elastic material behaviour. The edges at the transition between the two domains are coupled according to shell kinematics, so that spatial offsets in thickness direction are taken into account appropriately. This way, the number of degrees of freedom is reduced significantly and the computation of the impact response of large composite components is feasible within reasonable computational effort while failure mechanisms are modelled sufficiently detailed.

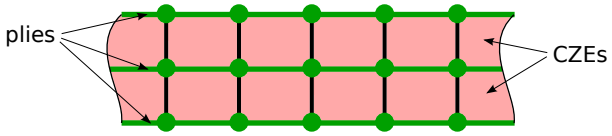

Figure 1. Schematic of a cross-section of the stacked shell approach (SSA). The plies are represented by the shell layers at the plies' mid-planes where the corresponding nodes are marked as dots. The CZEs are illustrated as shaded areas confined by black lines. [1]

Excerpt from ISBN 978-3-00-053387-7

When considering impact at component level, the assumption of a rigid impactor, typically taken when simulating the impact response at coupon specimen level, may no longer hold. The material behaviour of the impactor can influence the component's impact response and, hence, has to be taken into account. The present work considers impactors made from metallic materials. Their constitutive behaviour is modelled as elastic-plastic with isotropic strain hardening. In order to account for material failure within the impactor, a ductile damage approach is utilised.

3. Application Example

As an example, a composite fan containment casing of a jet engine subjected to fan blade out is investigated, cf. Fig. 2. The containment casing is of almost cylindrical shape with an average inner diameter of 834 mm and a width of 358 mm. The edge at the backside of the casing (+z direction) is fully clamped, whereas a free edge is modelled at the front side. The casing is made up of a quasi-isotropic glass fabric reinforced epoxy laminate where two configurations, one featuring 60 plies ($[(0_2/45_2/0_2)_5]_S$) and one featuring 80 plies ($[(0_2/45_2)_{10}]_S$), are considered. The nominal ply thickness is 0.254 mm and the nominal mass density is 2100 kg/m^3. The size of the highly resolved subsection (SSA-domain) is 210 mm in width and 93° in circumferential direction. The SSA is applied such that each shell layer represents two adjacent plies with equal orientation. The entire casing is discretised by linearly interpolated, fully integrated four-noded Mindlin-Reissner type shell elements. The embedding domain features an average element edge length of 5 mm. Within the SSA-domain, an average element edge length of 1 mm is assigned. The interfaces between individual shell layers within the SSA-domain are discretised by 8-noded, brick shaped CZEs.

The material parameters of the glass fabric/epoxy plies are listed in Tab. 1. The elastic constants and nominal strengths are taken from a corresponding material data sheet. The critical energy release rates are estimated from Ref. [5]. The shear behaviour is assumed. The properties of the interface are listed in Tab. 2. The initial stiffness is chosen so that a quasi-rigid connection between the plies is ensured before the emergence of delaminations. The mode II and mode III strengths are taken from a corresponding material data sheet, whereas the mode I strength is evaluated based on the mode II strength according to Ref. [6]. The critical energy release rates are taken from Ref. [7].

Four titanium fan blades (Ti6Al4V) are modelled where each blade features an average length of 219 mm,

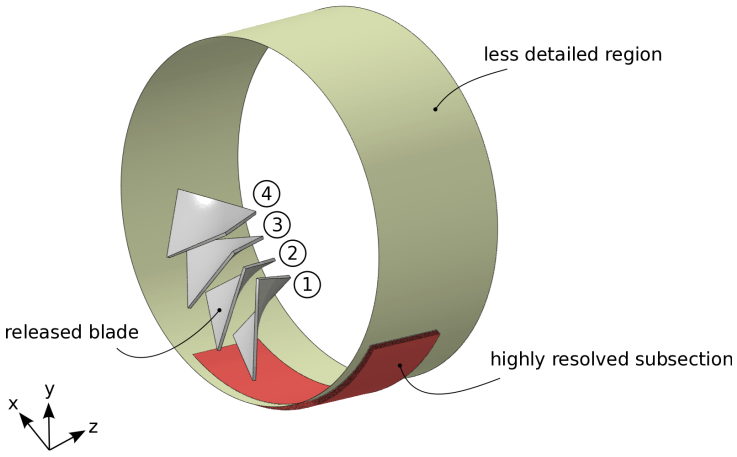

Figure 2. Simplified model of a jet engine fan blade containment casing. The subsection where impact is expected (red area) is modelled in high detail using a stacked shell approach.

Excerpt from ISBN 978-3-00-053387-7

Table 1. Material parameters of the glass fabric/epoxy plies. The subscript 1 and 2 denote the weft and warp directions, respectively. Details are given in [2] and [3].

elastic	E_1	E_2	ν_{12}	G_{12}	
constants	24 GPa	24 GPa	0.10825	4.8 GPa	
nominal	X_{1+}	X_{1-}	X_{2+}	X_{2-}	S_{12}
strengths	410 MPa	660 MPa	395 MPa	490 MPa	94 MPa
crit. energy	G_{Ic}^{1+}	G_{Ic}^{1-}	G_{Ic}^{2+}	G_{Ic}^{2-}	
release rate	65 N/mm	65 N/mm	65 N/mm	65 N/mm	
shear	α_{12}	$d_{12}^{\max}$	$\tilde{\sigma}_{\mathrm{y0}}$	C	p
behaviour	0.18634	1.0	55.0 MPa	669.94 MPa	0.823

Table 2. Parameters describing the initial stiffness of the interface, as well as damage initiation and propagation.

	Mode I	Mode II	Mode III
initial stiffnesses	10^6 N/mm^3	10^6 N/mm^3	10^6 N/mm^3
interlaminar strengths	35.07 MPa	68 MPa	68 MPa
crit. energy release rates	1.21 N/mm	4.55 N/mm	4.55 N/mm

Table 3. Material properties assigned to the fan blades. See the text for an explanation.

E	ν	σ_{y0}	$\bar{\varepsilon}_{\mathrm{f}}^{\mathrm{pl}}$	G_{f}	
113.8 GPa	0.342	700 MPa	0.1	5.0 N/mm	
σ_{yi}	831.6 MPa	865.5 MPa	880.0 MPa	896.8 MPa	917.8 MPa
$\bar{\varepsilon}_i^{\mathrm{pl}}$	0.02	0.05	0.07	0.1	0.15

an average width of 144 mm, an average thickness of 7 mm and a mass of 0.75 kg. The blades are rotating in negative z-direction with an initial speed of 11000 rpm. This results in an initial kinetic energy of 46 kJ for each blade. Blade number 2, cf. Fig. 2, is released whereas the other blades are rotating at constant speed throughout the fan blade out event. The blades are discretised by 8-noded, fully integrated, linearly interpolated three dimensional continuum elements. The released blade features an average element edge length of 1 mm while the other blades feature an average element edge length of 2 mm. The material parameters of the titanium blades are listed in Tab. 3. E and ν denote the Young's modulus and the Poisson ration and σ_{y0} the initial yield stress. The pairs of uniaxial tensile yield stresses, σ_{yi}, and equivalent plastic strains, $\bar{\varepsilon}_i^{\mathrm{pl}}$, define the hardening behaviour. Ductile damage is initiated at the equivalent plastic strain $\bar{\varepsilon}_{\mathrm{f}}^{\mathrm{pl}}$ and the corresponding critical energy release rate is denoted by G_{f}.

The contact constraints within the simulation are enforced using the general contact algorithm of Abaqus/Explicit, which utilises a penalty algorithm to compute contact forces. Contact is defined between each blade and every ply within the SSA-domain. As the trailing blades may collide with the released blade during the fan blade out event, contact between individual blades themselves is modelled. Additionally, contact between individual plies within the SSA-domain is modelled in order to maintain inter-ply contact in in regions of delamination, cf. [1].

4. Results and Discussion

In the following, the simulation results obtained with the presented modelling approach are discussed. Figures 3 and 4 show the deformation states of the two investigated configurations (60-plies vs. 80-plies) of the composite containment casing at 1.4 ms after the release of blade number 2. The SSA-domain

Excerpt from ISBN 978-3-00-053387-7

is depicted in yellow colour and the embedding domain in grey. The released blade is highlighted in red colour. As can be seen, the 60-ply casing undergoes severe damage and large cracks throughout the entire thickness of the laminate arise. The 80-ply casing exhibits significantly less damage compared to the 60-ply casing and the arising cracks don't propagate throughout the entire laminate thickness. In both cases, the trailing blade collides with the released blade and pushes it along the circumference of the casing. During this process, plastic deformations arise in both blades (blades number 2 and 3 in Fig. 2) and, at some point in time, material failure occurs within the released blade. In the case of the 60-ply configuration, the released blade and its fragments are markedly pushed outwards in radial direction and

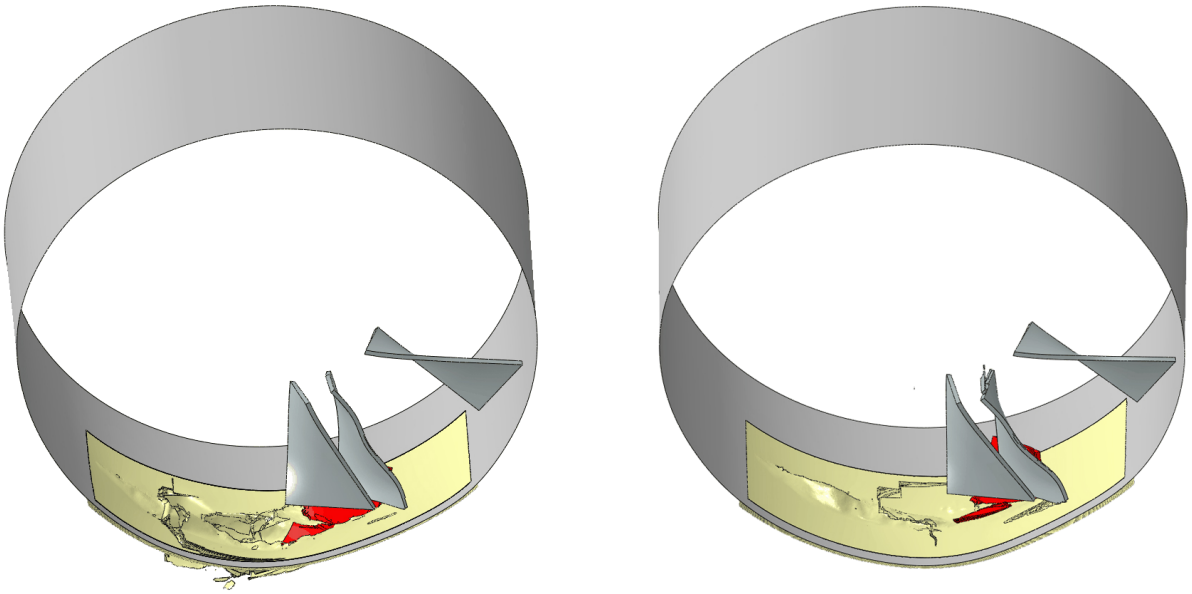

Figure 3. Inside view of deformed shape of the containment casing at 1.4 ms after blade release. The released blade is depicted in red. Left: 60-ply configuration. Right: 80-ply configuration.

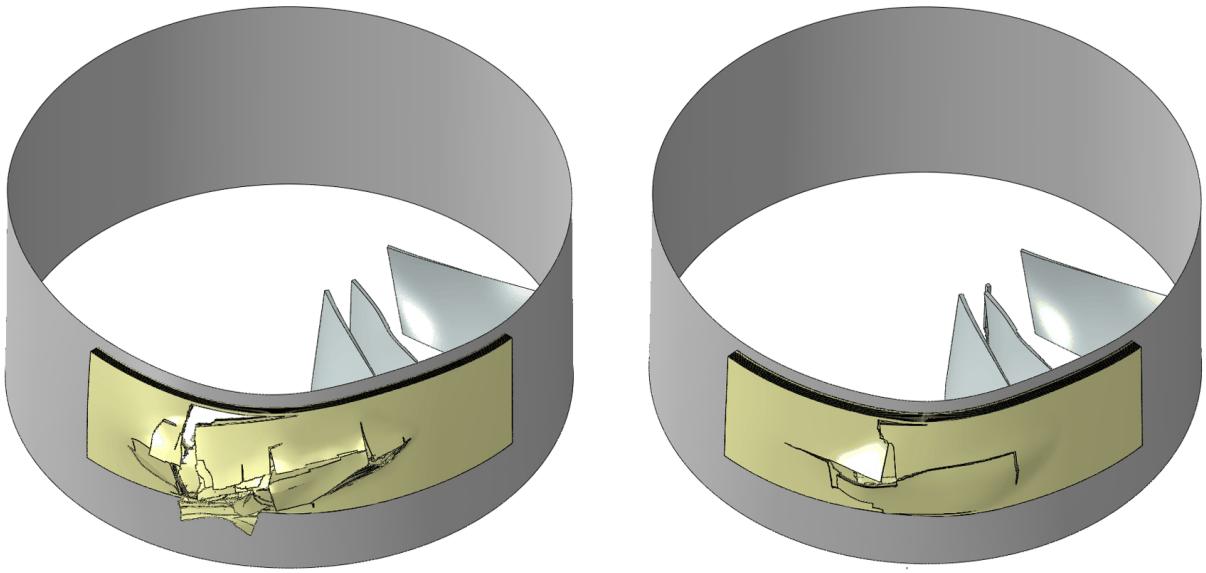

Figure 4. Outside view of deformed shape of the containment casing at 1.4 ms after blade release. The released blade is depicted in red. Left: 60-ply configuration. Right: 80-ply configuration.

Excerpt from ISBN 978-3-00-053387-7

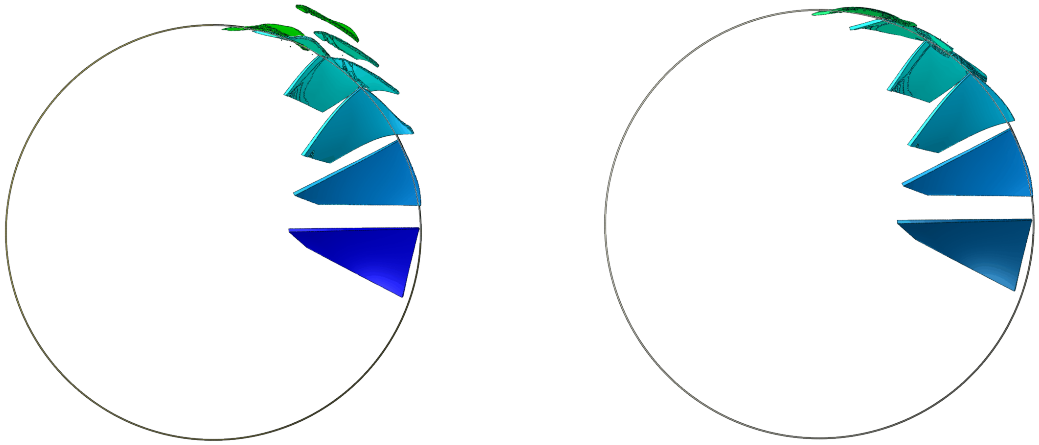

Figure 5. Time series of the position of the released blade in steps of 0.4 ms. The circle represents the inner diameter of the undeformed casing. Left: 60-ply configuration. Right: 80-ply configuration.

the residual stiffness of the severely damaged laminate is not high enough to keep the released blade contained within the casing, cf. Fig. 5 (left), where a time series of the position of the released blade is illustrated. In the case of the 80-ply casing, the initial impact of released blade is absorbed and its movement is redirected towards the back of the casing (downstream). From Fig. 5 (right) it can be concluded that the released blade is contained within the 80-ply casing.

The computations are conducted on a distributed memory cluster consisting of eleven standard PC workstations with, in total, 44 CPUs at 3.3 GHz. The 60-ply casing model features approximately 30 million degrees of freedom (DOFs) and the computation of the casing response for a time span of 2 ms takes 35 h. The 80-ply casing model features about 39 million DOFs and the simulation of 2 ms takes 49 h.

5. Summary

An efficient modelling strategy for simulating impact on structural components built from laminated composites is presented. The utilisation of a multiscale embedding approach in combination with shell element based discretisation allows the computational effort to be kept within reasonable bounds. Thereby, a highly resolved subsection is placed at the region where impact and associated material nonlinearities are expected to occur. Regions remote from the impact zone are modelled by a common laminate approach. The approach is demonstrated by investiganting a composite fan containment casing of a jet engine subjected to fan blade out. It is concluded that the proposed modelling approach is capable to simulate the impact response of large composite components within reasonable computation time and resources. Furthermore, it gives detailed information on the component's behaviour during the fan blade out event which includes the occurring damage modes and their extent. Such information helps to reduce the experimental effort associated with the design of impact loaded composite components and eventually leads to improvements their designs.

Acknowledgments

The funding within the framework of the TAKE OFF program by the Austrian Research Promotion Agency (FFG) and the Austrian Federal Ministry for Transport, Innovation and Technology is gratefully acknowledged.

Excerpt from ISBN 978-3-00-053387-7

References

[1] M Schwab, M Todt, M Wolfahrt, and HE Pettermann. Failure mechanism based modelling of impact on fabric reinforced composite laminates based on shell elements. *Composites Science and Technology*, 128:131–137, 2016.

[2] Dassault Systemes Simulia Corp., Providence, RI, USA. *VUMAT for Fabric Reinforced Composites, SIMULIA Answer 3749*, 2008.

[3] M. Schwab, M. Todt, and H. E. Pettermann. Simulation of the intermediate velocity impact behaviour of woven composite laminates applying progressive damage models for plies and interfaces. In O.T. Thomsen, C. Berggreen, and B.F. Sørensen, editors, *Proceedings of the 20th International Conference on Composite Materials, Paper-ID 4417-4*, 2015.

[4] Dassault Systemes Simulia Corp., Providence, RI, USA. *Abaqus Analysis User's Guide. Version 6.14*, 2014.

[5] G Caprino, V Lopresto, A Langella, and M Durante. Irreversibly absorbed energy and damage in gfrp laminates impacted at low velocity. *Composite Structures*, 93(11):2853–2860, 2011.

[6] A Turon, PP Camanho, J Costa, and J Renart. Accurate simulation of delamination growth under mixed-mode loading using cohesive elements: definition of interlaminar strengths and elastic stiffness. *Composite Structures*, 92(8):1857–1864, 2010.

[7] F Dharmawan, G Simpson, I Herszberg, and S John. Mixed mode fracture toughness of gfrp composites. *Composite Structures*, 75(1):328–338, 2006.

Excerpt from ISBN 978-3-00-053387-7